# One dimensional mathematical model for a thermocline energy storage device

HEIMO WALTER, NATALIE STROHMAYER, MICHAEL HAMETER
Institute for Energy Systems and Thermodynamics
TU-Wien
Getreidemarkt 9/302, 1060 Vienna
AUSTRIA
heimo.walter@tuwien.ac.at http://www.tuwien.ac.at/ite

*Abstract:* - The rapid rise of highly fluctuating renewables leads to challenges for power plants and power grids. Thermal energy storage is envisaged for e.g. enhancing the low load capabilities and plant dynamics of thermal power plants. As state of the art heat storage media like molten salts are rather expensive and furthermore limited due to their temperature range. In contrast a thermocline energy storage (TES) device is a cost efficient method to store thermal energy. Therefore a great interest is given on this technology. For time dependent studies of the integration of such a storage unit in complex energy systems a mathematical model is necessary. The model should be simple as possible to reduce the computation time for solving the algebraic equations of the model.
The objective of the paper is to present experimental data as well as a one-dimensional model for a thermocline energy storage unit. The measurements are done for a charging and discharging process. During the experiments the temperature and the mass flow of the heat transfer fluid (HTF) and also the temperature distribution within the storage device was measured.
For the time dependent TES model the energy balance for the storage mass and also for the heat transfer fluid (HTF) are discretised based on the finite volume approach. The measured HTF mass flow and entrance temperature into the TES are used as boundary condition for the simulation. The simulation results for the charging and discharging process of the TES test rig show a good agreement with the measured data.

*Key-Words:* - Thermocline, thermal energy storage, mathematical model, finite volume

## 1 Introduction

The conversion of the energy supply from the primary energy sources coal, oil, or gas to the renewable energy sources like wind, solar, etc. to achieve the ambitioned goals of the European Union to reduce the greenhouse gas emissions is characterized by the large volatility of these renewables. This volatility leads to challenges for the electrical power grid as well as for the operation of conventional power plants because the renewable energy sources require a high flexibility, rapidness, and adaptability. This relates to the situation that renewable energy, energy storage, and energy distribution will become one of the most important and strongly growing market for the next decades and hence also key topics for research and development. A dominant factor in the future energy scenario will be the energy storage. It can mitigate power variations, enhances the system flexibility, and enables the storage and dispatching of the electricity generated by variable renewable energy sources such as wind and solar [1]. The surplus energy can be stored in different ways like chemical or electrochemical, mechanical, electromagnetic or thermal storage, e.g. [2]-[8].

Thermal energy storage systems can be further subdivided into sensible (see e.g. [4], [6], [9]), latent (see e.g. [10], [11], [12]), and thermo-chemical storage (see e.g. [8], [13]) systems.

The present paper deals with a subarea of thermal energy storage: a thermocline energy storage (TES) device which is allocated to the group of sensible energy storage systems. The state-of-the-art design of this type of thermal storage is a vertical arranged vessel. But for some time it has been discussed also horizontal designs, see e.g. [14].

As described in [9], the thermocline energy storage device consists of a single tank filled with e.g. crushed rock as a cheap storage material forming a packed bed. The thermocline storage device is a simple, economically cost effective and efficient storage system. The main advantages of such a storage unit can be summarized as follows:

• applicable in a wide temperature range (only limited by the melting point of the storage material),

• operation close to ambient pressure,
• a direct contact heat transfer between working fluid and storage material,
• a mechanical and chemical long-term stability is given,
• a high reversibility between charging and discharging cycles,
• low environmental impact factors,
• no corrosion, degradation, and no-toxic, and
• storage material is cheap and available.

In addition, as it is reported in [15], a storage system with a single tank thermocline is about 35% cheaper than a system with two storage tanks. A similar result was found in [16]. The authors concluded that a 24% average reduction of TES investment costs could be reached by replacing conventional two-tank molten-salt storage with sensible rock-bed storage.

A Thermocline storage vessel underlies the principle of thermal stratification. This stratification is a result of the fluid having a temperature gradient under the action of gravitational force. The hot fluid is pushed upward by the bouncy force based on the lower density compared to the cold fluid, and the cold fluid is displaced downward. This behavior develops the vertical temperature profile which is called thermocline.

Early literature for TES systems was summarized by Garg et al. [17]. In this article also the work of Schuhmann [18] which has developed the first analyticle model of a rock bed thermal storage device. A remarkable work was presented by Coutier and Farber [19]. They presented empirical correlations for the heat transfer coefficient between the heat transfer fluid (HTF) air and the storage material rock. A comparison about various numerical models for packed bed storage units, both for sensible and phase change materials are presented by Ismail and Stuginsky [20]. The effect of axial dispersion and heat looses through the wall are analysed by Bindra et al. [21]. Based upon the temperature field modeling, recovered and lost exergy was calculated by the authors. The analysis has shown that, for packed beds, sensible heat storage systems can provide much higher exergy recovery as compared to phase change material storage systems under similar high temperature storage conditions. In [22] the same authors investigated the trade-off between thermal exergy losses and exergy losses through pressure loss. They concluded that the exergy recovery can improved by adding multiple inlets and outlets to the storage device according to the actual temperature profile.

In the following paragraph of the present paper the experimental setup and also the results of a measurement campaign at the TES unit located in the laboratory of the institute are presented.

After that a one dimensional model to calculate the transient behavior of a thermocline energy storage device will be presented. The model is suitable for integration into commercial available software to simulate and study time dependent complex energy sytems. The model is simple as possible to reduce the computation time for solving the algebraic equations of the model.

In a further paragraph the numerical results which are calculated with the presented model is compared with experimental data.

## 2 Experimental analysis

At the Institute for Energy Systems and Thermodynamics (IET) at TU-Wien a test rig for a thermocline energy storage device (see Fig. 1) was erected at the laboratory side of the institute.

### 2.1 Experimental test rig and instrumentation

A sketch of the test rig used for measuring the temperature distribution over the storage height and the pressure drop of the HTF air is shown in Fig. 1.

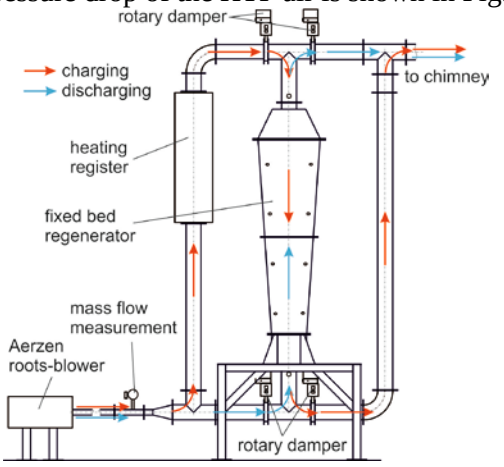


Figure 1: Sketch of the test rig

The TES device is equipped with a 15 kW electrical heating register which can heat up the air flow up to 330°C. The HTF is sucked by an Aerzen roots-blower (maximum pressure height of approx. 0,4 bar) from the ambient and flows through the thermal mass flow measuring system Proline t-mass A 150 from Endress+Hauser in direction to the heating register. Within the heating register the HTF is heated up to the requested inlet temperature of the TES. After leaving the heating register the hot HTF mass flow enters the thermocline vessel at the top and leaves the TES at the bottom in direction to the chimney (see red arrows in Fig. 1). During the flow

through the TES heat is released to the storage material. The discharging process is compared to the charging process characterized by a different HTF flow direction (see blue arrows in Fig. 1). The sucked air mass flow enters the TES unheated at the bottom and leaves the TES at the top in direction to the chimney.

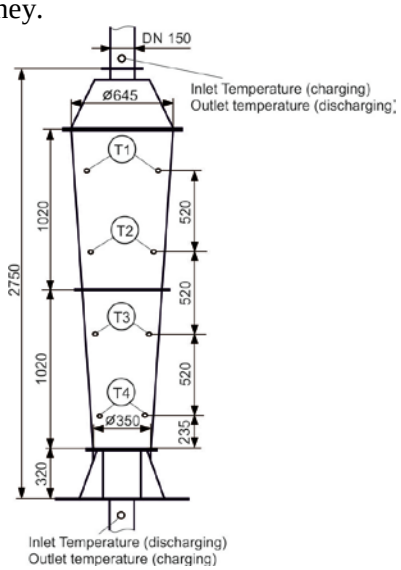


Figure 2: Dimensions of the test rig

Figure 2 presents the overall dimensions of the storage device as well as the locations of the calibrated NiCr-Ni thermocouples (type K, 4 pieces per layer T1 to T4). The storage vessel itself consists of three cone-shaped and one cylindrical steel rings whereby the later one is arranged at the bottom of the storage device. Only the two cone-shaped rings with a length of 1020 mm (see Fig. 2) are filled with the storage material. The storage vessel as well as the piping is insulated with mineral wool of a thickness of 200 mm. For experimental analysis the TES is filled with crushed rocks of a grain size between 30 to 72 mm.

A more detailed description of the test rig, the measurement instrumentation and uncertainties is provided in [23].

### 2.2 Measurement result

Figure 3 shows the temperature development over the TES height (Temperature T1 to T4) and the inlet and outlet temperature of the HTF as well as the air mass flow during the charging process. The mass flow of the HTF was constant at a averaged value of approx. 147,6 kg/h while the HTF inlet temperature increases rapidly from approx. 50°C to the maximum temperature of approx. 330°C. The total charging time was approx. 10h.

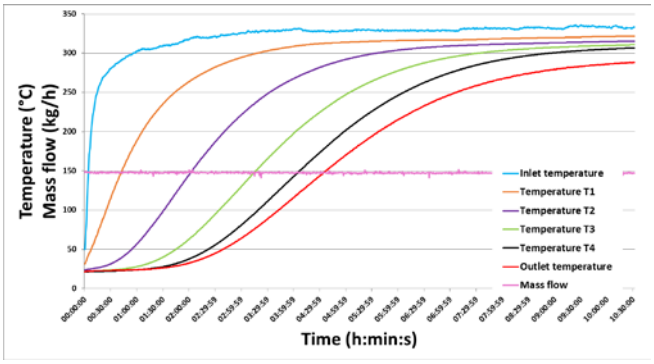


Figure 3: charging process: measured mass flow and temperature

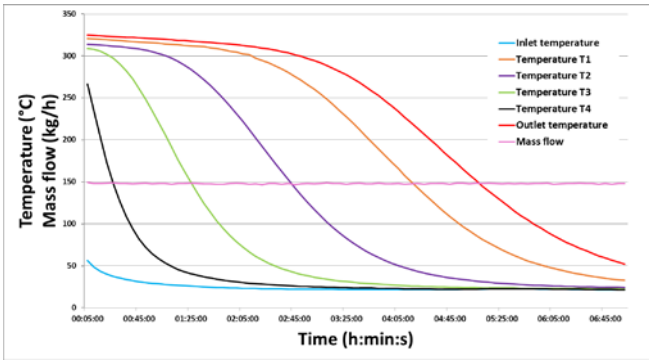


Figure 4: discharging process: measured mass flow and temperature

The time evolution of the storage material and air temperatures as well the air mass flow can be seen in Fig. 4 for the discharging process. Compared to the charging process a similar behavior by the development of the thermoclines during the discharging process is given within the TES. A comparison of the charging and discharging time shows that the discharging process is faster by approx. 180 minutes.

## 3 Numerical investigation

In the following the mathematical model, the physical properties as well as the boundary conditions used for the numerical simulation of the thermocline storage device will be presented.

### 3.1 Mathematical modelling

For the numerical simulation the balance equations for the solid (storage) material and the heat transfer fluid have to be solved in order to get the thermal behavior of the thermocline energy storage unit during the charging and discharging process. For the mathematical model some simplifying assumptions are made. In the following the most relevant assumptions are summarized:

- One-dimensional fluid flow and temperature distribution.
- Heat transfer from the HTF into storage material in radial direction.
- One-dimensional heat conduction in the storage material in axial direction.
- Packed bed with mono-dispersed particles and homogeneous distribution.
- Radiation heat transfer is neglected.
- Heat exchange between the storage unit and the surrounding is ignored (adiabatic vessel).
- Uniform temperature of the particles is assumed.
- The mass of the storage shell and the insulation is not taken into account to any thermal inertia.
- The change of the potential and kinetic energy of the HTF are neglected.
- The momentum balance for the HTF is reduced to a pressure balance.

### 3.1.1 Energy balance of the HTF

For the numerical simulation the TES was subdivided in axial direction into a higher number of control volumes and the energy balance equation was discretized using the Finite Volume method.

For a general control volume the discretized energy equation can be written as

$$a_{Pf,i}h_{f,i} = a_{Ef,i}h_{f,i+1} + a_{Wf,i}h_{f,i-1} + b_{f,i} \quad (1)$$

with the coefficients

$$a_{Ef,i} = \left[\left(\frac{\lambda_f}{c_{pf}}\right)_{i+1/2}\frac{1}{\Delta x_{i+1/2}} + MAX\left(\left(\varrho_f w\right)_{i+1/2}, 0\right)\right]A_{i+1/2} \quad (2)$$

$$a_{Wf,i} = \left[\left(\frac{\lambda_f}{c_{pf}}\right)_{i-1/2}\frac{1}{\Delta x_{i-1/2}} + MAX\left(\left(\varrho_f w\right)_{i-1/2}, 0\right)\right]A_{i-1/2} \quad (3)$$

$$a^0_{Pf,i} = \frac{\psi V_i \rho_i^0}{\Delta t} \quad (4)$$

$$a_{Pf,i} = a^0_{pf,i} + a_{Ef,i} + a_{Wf,i} - S_{pi}V_i \quad (5)$$

$$b_{f,i} = a^0_{pf,i}h^0 + S_{ci}V_i \quad (6)$$

$$S_{pi} = \frac{MAX(-\dot{Q}_{Vi},0)}{h_{f,i}} \quad (7)$$

$$S_{ci} = MAX\left(\dot{Q}_{Vi}, 0\right) \quad (8)$$

with the porosity

$$\psi = \frac{V_{Tot} - V_s}{V_{Tot}} \quad (9)$$

and the volume of the cell $i$:

$$V_i = \frac{\pi l}{3}\left(r^2_{i+1/2} + r_{i+1/2}r_{i-1/2} + r^2_{i-1/2}\right) \quad (10)$$

For the calculation of the heat transfer different forced convection correlations e.g. Coutier et al. [19], Wakao et al. [24], Singh et al. [25], and Gnielinski [26] are available in the open literature. As mentioned in [27] the heat transfer due to natural convection can be neglected compared to the forced convection heat transfer. In [28] a comparison between the correlations [19], [24], and [25] are presented. The authors concluded that there is no significant difference in the results for the temperature distribution within a fixed bed regenerator given. However, in the present study also a comparison between the correlation of Wakao et al. [24] and Gnielinski [26] will be presented.

- **Model of Wakao et al. [24]:**
  In the model of Wakoa et al. the volumetric convection heat transfer coefficient is calculated from Eq. (11).
  $$\alpha_V = \alpha_{sf}A_{sf} \quad (11)$$
  The heat transfer coefficient $\alpha_{sf}$ between the fluid and solid phase is given by
  $$\alpha_{sf} = \frac{\left(2+1{,}1Pr^{1/3}Re_p^{0.6}\right)\lambda_f}{d_p} \quad (12)$$
  For the specific surface area per volume $A_{sf}$, the correlation according to Vafai [29]
  $$A_{sf} = \frac{6(1-\psi)}{d_p} \quad (13)$$
  was applied. In Eq. (12) $Re_p$ denotes the particle Reynolds number and $Pr$ the Prandtl number. The definition region for the correlation is given by $Re_p$ = 15 to 8500.
- **Model of Gnielinski [26]:**
  For calculating the heat transfer coefficient between HTF and bulk material according to Gnielinski the Nusselt number
  $$Nu = \left(2 + \sqrt{Nu^2_{lam} + Nu^2_{turb}}\right)f_a \quad (13)$$
  has to be used. The Nusselt number is composed by a Nusselt number for the turbulent
  $$Nu_{turb} = \frac{0.037Re_p^{0.8}Pr}{1+2.443Re_p^{-0.1}\left(Pr^{2/3}-1\right)} \quad (14)$$
  and a laminar portion
  $$Nu_{lam} = 0.664\sqrt{Re_p}Pr^{1/3} \quad (15)$$
  The correction factor $f_a$ in Eq. (13) can be calculated with
  $$f_a = 1 + 1.5(1-\psi) \quad (16)$$

### 3.1.2 Energy balance of the solid

For a general control volume the discretized energy equation for the solid can be written as

$$a_{Ps,i}T_{s,i} = a_{Es,i}T_{s,i+1} + a_{Ws,i}T_{s,i-1} + b_{s,i} \quad (17)$$

with the coefficients

$$a_{Es,i} = \frac{A_{i+1/2}\lambda_{seff,i+1/2}}{(1-\psi)V_i\Delta x_{i+1/2}} \quad (18)$$

$$a_{Ws,i} = \frac{A_{i-1/2}\lambda_{seff,i-1/2}}{(1-\psi)V_i\Delta x_{i-1/2}} \quad (19)$$

$$a^0_{Ps,i} = \frac{\rho^0_i c^0_{pi}}{\Delta t} \quad (20)$$

$$a_{Ps,i} = \frac{\rho_i c_{pi}}{\Delta t} + a_{Es,i} + a_{Ws,i} \quad (21)$$

and

$$b_{s,i} = a^0_{ps,i}T^0 + \frac{\dot{Q}_{Vi}}{(1-\psi)} \quad (22)$$

The solid heat conduction in Eq. (18) and Eq. (19) is calculated as effective heat conduction according to [30]:

$$\lambda_{eff,i} = \frac{1}{\frac{\psi}{\lambda_f}+\frac{(1-\psi)}{\lambda_s}} \quad (23)$$

The energy balance for the solid and fluid phase are connected through the heat exchange and they are solved simultaneously.

### 3.1.3 Thermo-physical properties

In this study air is used as HTF. The thermo-physical properties for the HTF dry air are taken from [31].

The definition of the thermo-physical properties of the storage material is clouded with high uncertainties because the bulk material used in the study is commercial available crushed rock from the nearest surroundings to Vienna. As described in the literature [32] sedimentary rock, lime-sand brick, granite, lime stone, dolomite, and mica slate are the main hard rock formations around Vienna.

For the material under investigation no detailed material analysis is available and therefore the material composition is unknown. However, for the numerical simulation correlations from the literature for lime stone are applied.

The spec. heat capacity of rocks is temperature depending and usually increases with increasing temperature. As described in [33] the measured spec. heat capacity of rock samples have a high variation, and global literature data ranges from approx. 700 J/kgK to 1200 J/kgK. In the present study the correlation proposed by [34] was used in which the parameters are selected as mean values of different rock types [35]. The heat conduction of the rock stones was calculated by using the correlation presented in [36].

### 3.1.3 Boundary and initial conditions

At the edge of the computational grid time dependend boundary conditions must be set for the transient numerical simulation. At the entrance into the computational grid the mass flow and the temperature of the HTF was defined. The data for the inlet mass flow and the temperature of the HTF are taken from the experimental analysis which are presented in Fig. 3 and 4.

The initial condition for the charging process was set in such a way that the temperature in the computational grid (HTF and storage material) was set to 20°C and the fluid mass flow was set to zero while for the discharging process the temperature in the computational grid was set to the temperature distribution at the end of the charging process. The fluid mass flow at the beginning of the discharging process was identical to zero.

The numerical simulation was done for a porosity of $\psi$ = 0,337 (taken from the experimental setup).

## 4 Numerical results and discussion

Figure 5 and 6 presents the results of the numerical simulation for the charging and the discharging process for both analysed heat transfer correlations. The dotted lines show the simulation results calculated with the heat transfer correlation according to Gnielinski [26] while the dashed lines represents the result calculated with the correlation according to Wakoa et al. [24]. Within Fig. 5 and 6 the numerical results are compared with the measurement data (full line). The single graphs of the numerical results are utilized close to the layers where the thermocouples T1 to T4 are located in the test rig, see Fig. 2. Additional the HTF fluid temperature at the TES inlet as well as outlet are included in the figures.

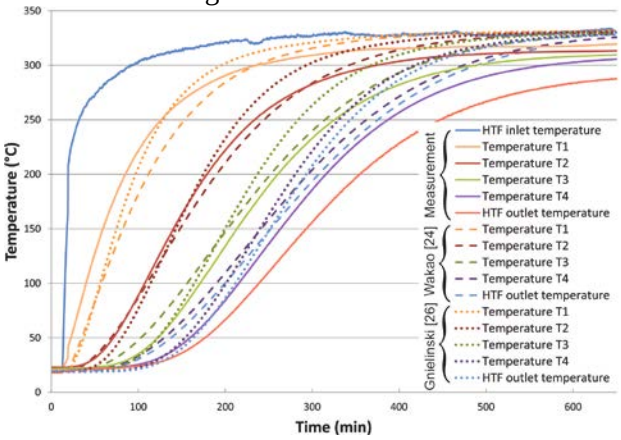


Figure 5: charging process: comparison between measured and simulated temperatures

A closer look to the charging process show that both correlation underestimates the measured data at storage temperatures smaller than approx. 250 to 300 °C (depending on the correlation). At higher temperatures both correlations overestimates the measured data.

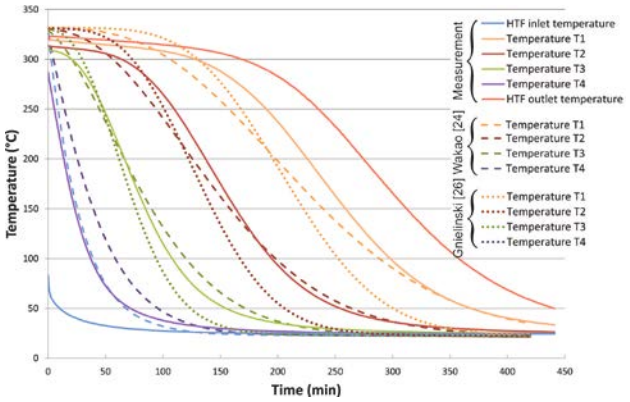

Figure 6: discharging process: comparison between measured and simulated temperatures

The same behavior can be seen during the discharging process.

The deviations between the simulated results and the measured data are a result of various effects:

- The model do not take into account the mass of the storage vessel (The ratio of storage material to vessel material (steel) is approx. 2). This results in a underestimation of the thermal storage capacity of the test rig during the simulations.
- The outer surface (curved surface area) to volume ratio is based on the dimensions of the test rig with approx. 15,8 very unfavorable. This results to higher heat flow losses compared to a storage vessel in industrial scale by same insulation. In the numerical simulations adiabatic conditions are assumed.
- As discussed above no detailed analysis of the thermo-physical properties of the storage material is available. This results also in deviations between the experimental and numerical data.

However, the overall characteristic of the TES can be represented in a good and fast way by the presented model. To improve the model two possibilities are open:

1) Including the heat flow looses into the model calculated with a thermal transmission coefficient.
2) Expanding the model to a 2-dimensional model. This will allow to take into account the storage vessel and insulation capacity as well as the heat looses. But this option is associated with a loos of computation speed.

# 5 Conclusion

The change of the energy supply away from the primary sources coal, oil and gas in direction to renewable sources is linked with the need for technologies to store and release energy dependent on the grid requirements. A thermocline energy storage, which counts to the sensible thermal energy storage technologies, can be part of the solution for this problem.

A one-dimensional model for the transient calculation of the thermocline energy storage device was presented in detail. The model was validated with measurement data based on calculations with two different heat transfer correlations. The numerical results show a good agreement with the experimental data.

The deviation between the measurement and numerical data are based on the unknown thermo-physical data of the storage material, the neglecting of the storage vessel mass and the unfavorable volume to surface ratio of the test rig which results in higher heat looses.

Suggestions for improving of the model are discussed.

# 6 Nomenclature

| | |
|---|---|
| $a$ | Discretisation coefficient |
| $A_{sf}$ | Specific surface area per volume (1/m) |
| $b$ | Constant term in discretisation equation |
| $c_p$ | Spec. heat at constant pressure (J/kg K) |
| $f_a$ | Correction factor (-) |
| $h$ | Spec. enthalpy (J/kg) |
| $l$ | Height of the TES (m) |
| $Nu$ | Nusselt number (-) |
| $Pr$ | Prandtl number (-) |
| $\dot{Q}_V$ | Heat flow per volume (W/m$^3$) |
| $r$ | Radius of TES (m) |
| $Re_P$ | Particle Reynolds number (-) |
| $S_P$ | Constant term of the linearized source term |
| $S_P$ | Proportional term of the linearized source term |
| $t$ | Time (s) |
| $T$ | Temperature (K) |
| $w$ | Velocity (m/s) |
| $x$ | Length (m) |
| $\Delta x$ | Increment in space (m) |

Greek letters

| | |
|---|---|
| $\alpha_{sf}$ | Heat transfer coefficient (W/m$^2$K) |
| $\alpha_V$ | Volumetric heat transfer coefficient (W/m$^3$K) |
| $\vartheta$ | Temperature (°C) |
| $\lambda$ | Thermal conductivity (W/m K) |
| $\rho$ | Density (kg/m$^3$) |
| $\psi$ | Porosity |

Subscripts

| | |
|---|---|
| *eff* | Effective |
| *E* | East grid point |
| *f* | Fluid |
| *i* | counter |
| *lam* | laminar |
| *p* | Particle |
| *P* | Grid point |
| *s* | Solid |
| *sf* | Solid/Fluid |
| *turb* | Turbulent |
| *Tot* | Total |
| *V* | Volume |
| *W* | West grid point |

**Acknowledgments**

The K-Project GSG-GreenStorageGrid (grand number 836636) is funded in the framework of COMET - Competence Centers for Excellent Technologies by the Federal Ministry of Transport, Innovation and Technology, the Federal Ministry of Science, Research and Economy, the Vienna Business Agency, the Federal Province of Lower Austria and by the Federal Province of Upper Austria. The program line COMET is administered by the Austrian Research Promotion Agency (FFG).

*References:*

[1] S. Ould Amrouche, D. Rekioua, T. Rekioua, and S. Bacha, Overview of energy storage in renewable energy systems, *International Journal of Hydrogen Energy*, Vol. 41, No. 45, 2016, pp. 20914 – 20927.

[2] S. Aissou, D. Rekioua, N. Mezzai, T. Rekioua and, S. Bacha, Modeling and control of hybrid photovoltaic wind power system with battery storage, *Energy Conversion and Management*, Vol. 89, 2015, pp. 615 – 625.

[3] A. De Gracia and L. F. Cabeza, Phase change materials and thermal energy storage for buildings, *Energy Build*, Vol. 103 2015; pp. 414 - 419.

[4] P. Steiner, K. Schwaiger, M. Haider, and H. Walter: System analysis of central receiver concepts with high temperature thermal energy storages: Receiver technologies and storage cycles, *AIP Conference Proceedings - American Institute of Physics*, Vol. 1850, 2017, pp. 110015-1 - 110015-8.

[5] Guruprasad Alva, Yaxue Lin, and Guiyin Fang, An overview of thermal energy storage systems, *Energy*, Vol. 144, 2018, pp. 341 – 378.

[6] V. Becattini, L. Geissbühler, G. Zanganeh, A. Haselbacher, and A. Steinfeld, Pilot-scale demonstration of advanced adiabatic compressed air energy storage, Part 2: Tests with combined sensible/latent thermal-energy storage, *Journal of Energy Storage*, Vol. 17, 2018, pp. 140 – 152.

[7] C. Bauer, E. Doujak. Aktueller Stand zur Entwicklung einer modularen Pumpturbine im niedrigen Leistungsbereich. *Wasserwirtschaft*, Vol. 107, No. 10, 2017, pp. 54 – 58.

[8] S. Flegkas, F. Birkelbach, F. Winter, N. Freiberger, and A. Werner, Fluidized bed reactors for solid-gas thermochemical energy storage concepts - Modelling and process limitations, *Energy*, Vol. 143, 2018, pp. 615 – 623.

[9] F. Mayrhuber, H. Walter, and M. Hameter, Experimental and Numerical Investigation on a Fixed Bed Regenerator, in: "Proceedings of the 10th International Conference on Sustainable Energy and Environmental Protection", University of Maribor Press, (2017), Bled, Slovenia; 27.06.2017 - 30.06.2017, pp. 14.

[10] C. Zauner, F. Hengstberger, B. Mörzinger, R. Hofmann, and H. Walter, Experimental characterization and simulation of a hybrid sensible-latent heat storage, *Applied Energy*, Vol. 189, 2017, pp. 506 - 519.

[11] M. Koller, H. Walter, and M. Hameter, Transient Numerical Simulation of the Melting and Solidification Behavior of NaNO3 Using a Wire Matrix for Enhancing the Heat Transfer, *Energies*, Vol. 9, No. 205, 2016, pp. 1 - 18.

[12] H. Walter, A. Beck, and M. Hameter, Influence of the Fin Design on the Melting and Solidification Process of NaNO3 in a Thermal Energy Storage System, *Journal of Energy and Power Engineering*, Vol. 9, No. 11, 2015, pp. 913 - 928.

[13] M. Deutsch, F. Birkelbach, C. Knoll, M. Harasek, A. Werner, and F. Winter, An extension of the NPK method to include the pressure dependency of solid state reactions, *Thermochimica Acta*, Vol. 654, 2017, pp. 168 - 178.

[14] M. Prenzel, V. Danov, S. Will, L. Zigan, T. Barmeier, J. Schäfer, Thermo-fluid dynamic model for horizontal packed bed thermal energy storages, *Energy Procedia*, Vol. 135, 2017, pp. 51- 61.

[15] D. Brosseau, J. W. Kelton, M. Edgar, K. Chisman, and B. Emms, Testing of thermocline filler materials and molten-salt heat transfer fluids for thermal energy storage systems in parabolic trough power plants, *Transaction of*

*ASME Journal of Solar Energy Engineering*, Vol. 127, 2005 pp. 109 – 116.

[16] E. P. R. Institute, Solar Thermocline Storage Systems: Preliminary Design Study, Tech. Rep. 1019581, Electric Power Research Institute, 2010.

[17] H. P. Garg, S. C. Mullick, A. K. Bhargava, *Solar Thermal Energy Storage*, D. Reidel, Publishing Company, Dordrecht, 1985.

[18] T. Schumann, Heat transfer: a liquid flowing through a porous prism, *Journal of the Franklin Institute*, Vol. 208, 1929, pp. 405 – 416.

[19] J. Coutier, E. Farber, Two applications of a numerical approach of heat-transfer process within rock beds, *Solar Energy*, Vol. 29, No. 6, pp. 451-462, 1982.

[20] K. Ismail, R. Stuginsky, A parametric study on possible fixed bed models for pcm and sensible heat storage, *Applied Thermal Engineering*, Vol. 19, No. 7, 1999, pp. 757 - 788.

[21] H. Bindra, P. Bueno, J. F. Morris, R. Shinnar, Thermal analysis and exergy evaluation of packed bed thermal storage systems, *Applied Thermal Engineering*, Vol. 52, No. 2, 2013, pp. 255 – 263.

[22] H. Bindra, P. Bueno, J. F. Morris, R. Shinnar, Sliding flow method for exergetically efficient packed bed thermal storage, *Applied Thermal Engineering*, Vol. 64, 2014, pp. 201 – 208.

[23] P. Drochter, Design, construction and errection of a fixed bed regenerator, MS-thesis, TU-Wien, 2016 (in German).

[24] N. Wakao, S. Kaguei, T. Fuazkri, Effect of fluid dispersion coefficients on particle-to-fluid heat transfer coefficients in packed beds, *Chemical Engineering Science*, Vol. 34, pp. 325-336, 1979.

[25] S. R. P. H. Singh, J. Saini, Performance of a packed bed solar energy storage system having large sized elements with low void fraction, *Solar Energy*, Vol. 87, pp. 22-34, 2013.

[26] V. Gnielinski, Wärme- und Stoffüber-tragung in Festbetten, *Chemie Ingenieur Technik*, Vol. 52, No.: 3, 1980, pp. 228 – 236.

[27] M. Hänchen, S. Brückner, A. Steinfeld, High-temperature thermal storage using a packed bed of rocks e heat transfer analysis and experimental validation, *Applied Thermal Engineering*, Vol. 31, 2011, pp. 1798 – 1806.

[28] F. Mayrhuber, H. Walter, M. Hameter, Experimental and numerical investigation on a fixed bed regenerator, *Proceedings of the 10th International Conference on Sustainable Energy and Environmental Protection*, University of Maribor Press, 2017.

[29] K. Vafai, M. Sözen, Analysis of energy and momentum transport for fluid flow through a porous bed, *Journal of Heat Transfer*, Vol. 112, pp. 690-699, 1990.

[30] M. Hänchen, S. Brückner and A. Steinfeld, High-temperature thermal storage using a packed bed of rocks – heat transfer analysis and experimental validation, *Applied Thermal Engineering*, Vol. 31, Nr.10, 2011 pp. 1798-1806.

[31] F. Brandt, *Wärmeübertragung in Dampf-erzeugern und Wärmeaustauschern*. 2. edn. Vulkan, 1995.

[32] M. Heinrich, *Bundesweite Übersicht zum Forschungsstand der Massenrohstoffe Kies, Kiessand, Brecherprodukte und Bruchsteine für das Bauwesen hinsichtlich der Vorkommen, der Abbaubetriebe und der Produktion sowie des Verbrauches - Niederösterreich, Wien und Burgenland*, interim report Projekt ÜLG 26/1990, Berichte der Geologischen Bundesanstalt, Heft 29, 1995.

[33] V. Cermak, H. G. Huckenholz, L. Rybach, R. Schmid, J. R. Schopper, M. Schuch, D. Stöffler, J. Wohlenberg: *Landtolt-Börnstein – Zahlenwerte und Funktionen aus Naturwissenschaften und Technik, Gruppe V Geophysik und Weltraumforschung*, Volume 1 Physikalische Eigenschaften der Gesteine, Springer Verlag, Berlin Heidelberg, 1982.

[34] K. Kelley, Contribution to the data on theoretical metallurgy: XIII. high-temperature heat-content, heat-capacity, and entropy data for the elements and inorganic compounds, U.S. Government Printing Office, Washington, 1960.

[35] G. Zanganeh, A. Pedretti, S. Zavattoni, M. Barbato, A. Steinfeld, Packed-bed thermal storage for concentrated solar power – Pilot-scale demonstration and industrial-scale design, *Solar Energy*, vol. 86, pp. 3084-3098, 2012.

[36] W. H. Somerton, Thermal properties and temperature-related behaviour of rock/fluid systems, series in Developments in Petroleum Science, Elsevier, vol. 37, 1st. edition 1992.